DOI 10.5012/bkcs.2010.31.5.1267

Electrochemical Characteristics of Lithium Vanadium Oxide for Lithium Secondary Battery

Hyung Sun Kim* **and Byung Won Cho**

*Advanced Battery Center, Korea Institute of Science and Technology (KIST), P.O. Box, 131, Cheongryang, Seoul 130-650, Korea. *E-mail: kimhs@kist.re.kr*
Received November 5, 2009, Accepted March 10, 2010

The pure crystalline $Li_{1.1}V_{0.9}O_2$ powder has been prepared by a simple solid state reaction of Li_2CO_3 and V_2O_3 precursors under nitrogen gas containing 10 mol % hydrogen gas flow. The structure of $Li_{1.1}V_{0.9}O_2$ powder was analyzed using X-ray diffraction (XRD) and scanning electron microscope (SEM). The stoichiometric $Li_{1.1}V_{0.9}O_2$ powder was used as anode active material for lithium secondary batteries. Its electrochemical properties were investigated by cyclic voltammetry and constant current methods using lithium foil electrode. The observed specific discharge capacity and charge capacity were 360 mAh/g and 260 mAh/g during the first cycle, respectively. In addition, the cyclic efficiency of this cell was 72.2% in the first cycle. The specific capacity of $Li_{1.1}V_{0.9}O_2$ anode rapidly declines as the current rate increases and retains only 30 % of the capacity of 0.1C rate at 1C rate. The crystallinity of the $Li_{1.1}V_{0.9}O_2$ anode decrease as discharge reaction proceeds. However, the relative intensity of main peaks was almost recovered when the cell was charged up to 1.5 V.

Key Words: Lithium vanadium oxide, Anode material, Lithium battery

Introduction

Recently, the development of new vanadium-based anode materials for lithium secondary battery has been introduced to meet the requirement for portable power sources with high energy density.[1-7] Among these materials, lithium vanadium oxide ($Li_{1.1}V_{0.9}O_2$) has attracted considerable attention because of its high specific capacity per unit volume and low working potential below 0.3 V *vs*. Li/Li^+ compared with other transition metal-based material. The theoretical specific capacity of this material is about 1200 $mAhcm^{-3}$, which corresponds to approximately 1.8 times greater than commercial available graphite material. In addition, it is expected that this anode shows a better cycling performance in comparison with other anode materials because it accompanies a smaller volume change during the cycling.[8] To date, it has also been reported that further research on the structure and valence state of this material would be promising due to its potential anode application.[9,10] However, it is very difficult to prepare the pure $Li_{1.1}V_{0.9}O_2$ anode material because the valence state of vanadium-based material can be easily changed during the solid state reactions at high temperature. Therefore, it is necessary to avoid the formation of impurity such as Li_3VO_4 material during the sintering process. In the present work, we report a simple preparation method to obtain the pure crystalline stoichiometric $Li_{1.1}V_{0.9}O_2$ anode material and investigate its electrochemical properties using various electroanalytical techniques.

Experimental

$Li_{1.1}V_{0.9}O_2$ anode material was prepared by a solid-state reaction method. The stoichiometric amounts of Li_2CO_3 (Aldrich, 98%) and V_2O_3 (Alfa Aesar, 99.7%) were ball-milled in a planetary machine (Pulverisette 7, Fritsch) at a rotation speed of 250 rpm for 1h. Then, the ball-milled powders were sintered at 1100 ^oC for 8h under N_2 gas flow containing 10 mol % H_2 and naturally cooled down to room temperature. The structure of obtained powder was characterized by X-ray diffraction (XRD, Rint/Dmax-2500, Rigaku) using Cu Kα radiation and scanning electron microscope (SEM, Hitachi 4200, Japan). The procedure of $Li_{1.1}V_{0.9}O_2$ anode fabrication was as follows. $Li_{1.1}V_{0.9}O_2$ active material, poly (vinylidene fluoride) (8 wt % in *N*-methyl pyrrolidinone solvent) binder and carbon black conductive agent were mixed in homogenizer at 3,000 rpm for 1 h with a weight percent ratio of 90 : 5 : 5, respectively. Then, the slurry was cast onto copper foil by a doctor-blade method and dried at 80 ^oC in vacuum oven for 24 h. The electrochemical behavior of this anode was investigated under the following steps. $Li_{1.1}V_{0.9}O_2$ anode was assembled with lithium foil electrode using CR2032 coin cells in a dry room. A microporous polypropylene membrane (Celgard 2400) was used as a separator. The electrolyte used was 1M $LiPF_6$ in a mixed solvent of ethylene carbonate and diethyl carbonate (3:7 by volume ratio). The cells were tested using galvanostatic and cyclic voltammetry methods in the voltage range from 0.005 to 1.5 V *vs*. Li/Li^+ by Maccor cycle system (S4000, USA).

Results and Discussion

Fig. 1 compares the XRD patterns of the $Li_{1.1}V_{0.9}O_2$ powder prepared at 1100 ^oC under N_2 gas flow with 10 mol % H_2 (sample A) or without H_2 gas (sample B), respectively. The crystal structure of $Li_{1.1}V_{0.9}O_2$ powders could be assigned to the hexagonal structure with a *R*-3*m* space group with cell parameters of a = 2.853 Å and c = 14.698 Å.[11] The powder pattern of the sample A is similar to that of sample B that obtained in pure N_2 gas flow. However, the peaks corresponded on Li_3VO_4 materials were diminished by reduction atmosphere. Hereafter the sample A

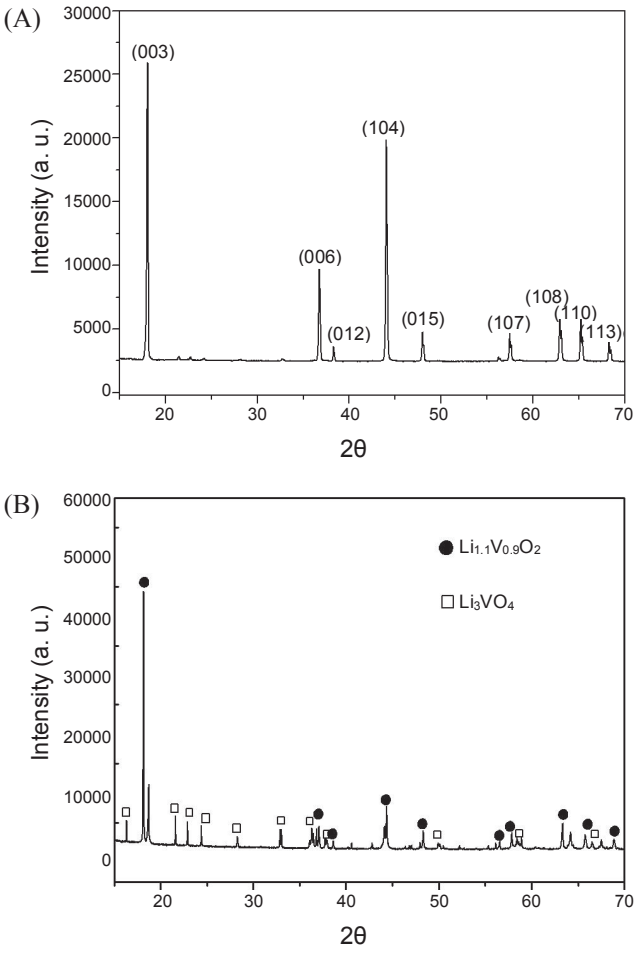

Figure 1. XRD patterns of the synthesized $Li_{1.1}V_{0.9}O_2$ powder under N_2 containing 10 mol % H_2 (A) and pure N_2 (B) gas flow.

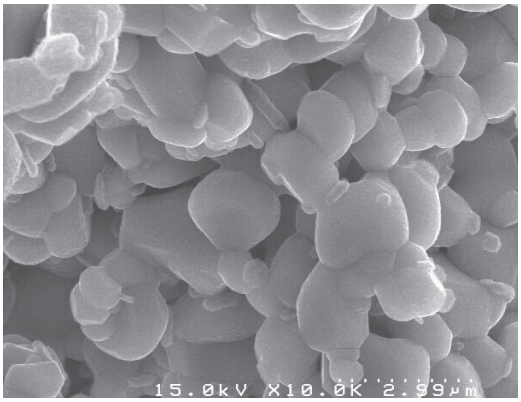

Figure 2. SEM image of the synthesized $Li_{1.1}V_{0.9}O_2$ powder.

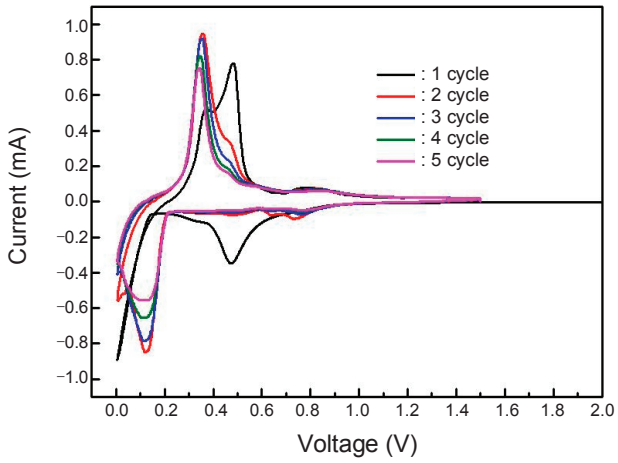

Figure 3. Cyclic voltammogram of $Li_{1.1}V_{0.9}O_2$ anode at room temperature.

was used as anode material to investigate its electrochemical properties. Fig. 2 shows the SEM image of the $Li_{1.1}V_{0.9}O_2$ powder obtained by solid-state reaction. The morphology of the particle was a spherical feature and the mean diameter was approximately 1 μm or greater. The cyclic voltammogram of $Li_{1.1}V_{0.9}O_2$ anode is shown in Fig. 3, at a scan rate of 0.5 mV/sec, recorded at room temperature. During the first cathodic scan (lithium intercalation), the electrode shows a well resolved intense peak at 0.48 V and the second peak around 0.1 V on further intercalation. During the first anodic scan (lithium deintercalation), two sharp peaks around 0.38 V and 0.48 V are clearly observed. From the second cycle, the first cathodic current peak at 0.48 V do not appear and the main lithium intercalation peaks begin at 0.2 V. This result indicates that the first cathodic current peak can be related to the irreversible capacity such as structural change and solid electrolyte interphase (SEI) formation. In the subsequent cycles, the cathodic and anodic peaks voltages are almost at the same position. The cathodic and anodic current peak ratios are also in the range of 0.8 ~ 1.2. This means that the intercalation reaction is reversible or quasi-reversible. Fig. 4 shows the charge-discharge voltage profiles of the stoichiometric $Li_{1.1}V_{0.9}O_2$ anode conducted by galvanostatic mode in the potential range of 0.005 and 1.5 V. During the initial lithium intercalation, the voltage dramatically decreased to ~ 0.58 V from the open circuit voltage (~ 3.0 V) followed by the first plateau potential about 0.58 V and the second plateau about 0.1 V at 0.1 C rate, respectively. This is in good agreement with the previous results of cyclic voltammetry. After that, the cell voltage decreases continuously till it reaches 0.005 V whereas one plateau in the potential ranges of 0.3 V ~ 0.5 V is seen during lithium de-intercalation reaction. The observed discharge capacity and charge capacity values during the first cycle were 360 mAh/g and 260 mAh/g, respectively. The cyclic efficiency of this cell was 72.2% in the first cycle. From the next cycle, although the cycle efficiency increased to 92.2% due to the disappearance of side reaction, the specific capacity decreased continuously as cycling proceeds. It can be considered that lithium ions inserted in $Li_{1.1}V_{0.9}O_2$ can not move reversibly to form $Li_{1.1+x}V_{0.9}O_2$ (x = 0 ~ 1). The remaining lithium ions cannot be completely extracted by electrochemical method. Fig. 5 shows the charge-discharge voltage profiles of the same $Li_{1.1}V_{0.9}O_2$ anode in the potential range of 0.005 and 1.5 V at various current rates. As expected, the anode shows maximum initial capacity at the lowest current rate. With increasing current rate, the charge potential plateau drops slightly, indicating an increased polarization caused by the hindered electrochemical kinetics in the electrode intercala-

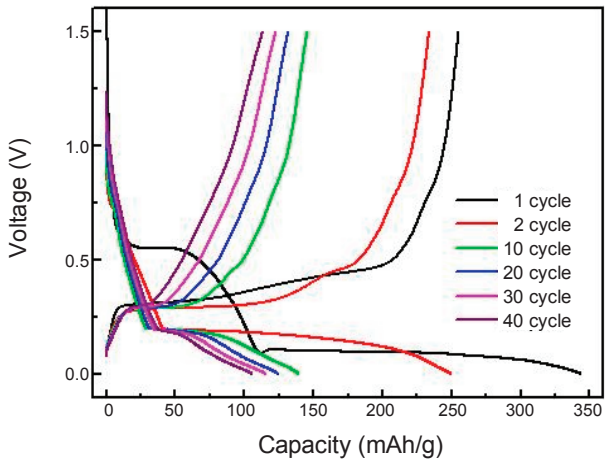

Figure 4. Charge/discharge curves of $Li_{1.1}V_{0.9}O_2$ anode with cycle number.

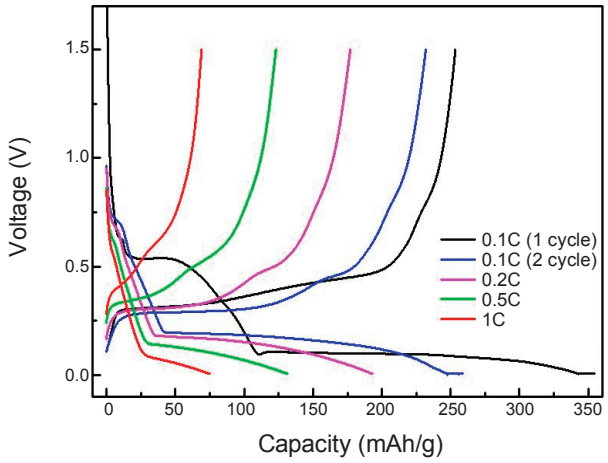

Figure 5. Charge/discharge curves of $Li_{1.1}V_{0.9}O_2$ anode at various rates.

tion reaction. The specific capacity of $Li_{1.1}V_{0.9}O_2$ anode rapidly declines as the current rate increases and retains only 30% of the capacity of 0.1 C rate at 1 C rate. This effect can be ascribed to the low electrical conductivity of the $Li_{1.1}V_{0.9}O_2$ active material. Fig. 6 shows the XRD patterns of the $Li_{1.1}V_{0.9}O_2$ anode before and after cycling test, respectively. According to the XRD result, the crystallinity of the $Li_{1.1}V_{0.9}O_2$ anode decrease as discharge reaction proceeds. When the cell is fully discharged up, the structure of $Li_{1.1}V_{0.9}O_2$ anode changed into $Li_{2.1}V_{0.9}O_2$, corresponded to *P*-3*m*1 space group with cell parameters of a = 3.099 Å, c = 5.212 Å[11] and the oxidation valence number of vanadium also changes from V^{+3} to V^{+2} during the discharge reaction. In addition, the peak (104) and the intensity of other main peaks in the XRD patterns were split into two peaks and decreased due to the structural transformation during the lithium intercalation, respectively. However, the relative intensity of this peak and other main peaks were almost recovered when the cell was charged up to 1.5 V. This result suggests that the phase stability of $Li_{2.1}V_{0.9}O_2$ anode arises from the homogeneous distribution of the pure crystalline active material in the electrode.

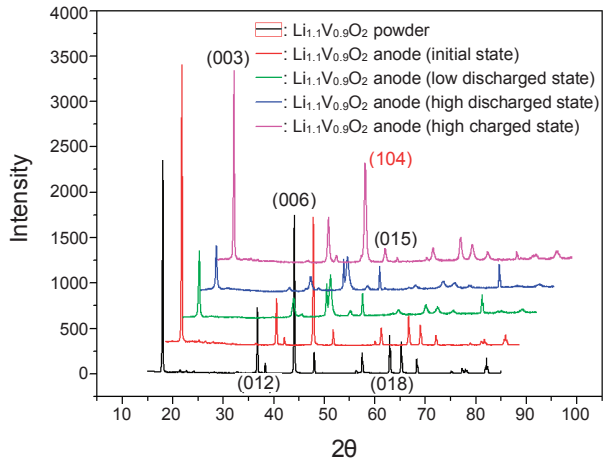

Figure 6. XRD patterns of the $Li_{1.1}V_{0.9}O_2$ anode before and after cycle test at 0.1C rate.

Conclusions

The crystalline $Li_{1.1}V_{0.9}O_2$ powder has been prepared by a simple solid state reaction under nitrogen gas containing 10 mol % hydrogen gas flow. From the XRD results, we obtained the stichiometric $Li_{1.1}V_{0.9}O_2$ powder without other impurities such as Li_3VO_4. $Li_{1.1}V_{0.9}O_2$ anode showed the specific discharge capacity and charge capacity of 360 mAh/g and 260 mAh/g during the first cycle, respectively. The specific capacity of $Li_{1.1}V_{0.9}O_2$ anode rapidly declines as the current rate increases and retains only 30% of the capacity of 0.1C rate at 1C rate. Even though the crystallinity of the $Li_{1.1}V_{0.9}O_2$ anode decrease as discharge reaction proceeds, the relative intensity of main peaks was recovered when the cell was charged up to 1.5 V.

Acknowledgments. This work was supported financially by "The Middle and Long-term Technology Development Project" of the Ministry of Knowledge Economy in Korea.

References

1. Denis, S.; Baudrin, E.; Touboul, M.; Tarascon, J-M. *J. Electrochem. Soc.* **1997**, *144*, 4099.
2. Kim, S.; Ikuta, H.; Wakihara, M. *Solid State Ionics* **2001**, *139*, 57.
3. Morishita, T.; Nomura, K.; Inamasu, T.; Inagaki, M. *Solid State Ionics* **2005**, *176*, 2235.
4. Reddy, M.; Pecquenard, B.; Vinatier, P.; Levasseur, A. *Electrochemistry Communications* **2007**, *9*, 409.
5. Bhuvaneswari, M.; Selvasekarapandian, S.; Kamishima, O.; Kawamura, J.; Hattori, T. *J. Power Sources* **2005**, *139*, 279.
6. Kim, H.; Chung, K.; Cho, W.; Cho, B. *Bulletin of the Korean Chemical Society* **2009**, *30*, 1607.
7. Kim, H.; Chung, K.; Cho, B. *J. Power Sources* **2009**, *189*, 108.
8. Kim, S.; Kim, J.; Koike, M.; Kobayashi, N. *Abstract No. 20 of the 14th International Meeting on Lithium Batteries*; Tianjin, China, June 22-28, 2008.
9. Yamamoto, H.; Higashida, Y.; Kitano, A. *The 43rd Battery Symposium in Japan* **2002**, 3B05.
10. Kim, S.; Kim, J.; Koike, M.; Kobayashi, N. *The 48th Battery Symposium in Japan* **2007**, 2F06.
11. Yin, R.; Kim, Y.; Choi, W.; Kim, S.; Kim, H. *Advances in Quantum Chemistry* **2008**, *54*, 23.